

Nanostructured Ga doped ZnO thin films prepared by Sol-Gel spin-Coating

Filmes finos de ZnO Nanoestruturados Ga doped preparados por sol-Gel spin-Coating

DOI:10.34117/bjdv7n12-144

Recebimento dos originais: 12/11/2021

Aceitação para publicação: 06/12/2021

Claudia Daniela Bojorge

Dra en Ciencia y Tecnología de los Materiales

UNIDEF (Unidad Ejecutora MINDEF-CONICET-CITEDEF)

Juan Bautista de La Salle 4397, Villa Martelli, B1603ALO - Pcia. de Buenos Aires –
Argentina

cbojorge@citedef.gob.ar , bojorgeclau@gmail.com

Horacio Ricardo Cánepa

Dr. en Ciencias Físicas

UNIDEF (Unidad Ejecutora MINDEF-CONICET-CITEDEF)

Juan Bautista de La Salle 4397, Villa Martelli, B1603ALO - Pcia. de Buenos Aires –
Argentina

canepaster@gmail.com

Eduardo Armando Heredia

Licenciado en Ciencias Física

UNIDEF (Unidad Ejecutora MINDEF-CONICET-CITEDEF)

Juan Bautista de La Salle 4397, Villa Martelli, B1603ALO - Pcia. de Buenos Aires –
Argentina

eheredia@citedef.gob.ar , heredia.edu@gmail.com

ABSTRACT

ZnO nanostructures are used in device systems such as photodetectors, gas sensors, photoemission devices, UV-photosensors and many others in Optoelectronics. In the present work we studied nanocrystalline ZnO:Ga thin films prepared by the sol-gel dip-coating technique. Samples were characterized by Grazing Incidence X-ray Diffraction (GIXD), X-ray Reflectivity (XR) and Grazing Incidence Small-Angle X-ray Scattering (GISAXS) methods and Field Effect Scanning Electronic Microscopy (FESEM). Characterization of the samples shows that the obtained films were uniform, continuous, with a crystallite size around 12 nm, an average pores size of around 3.5 nm, and a volume fraction of nanoporosity between 0.18 and 0.3. Comparison of densities between doped and undoped films is discussed.

Keywords: ZnO:Ga, nanocrystalline films, GISAXS, XR.

RESUMO

As nanoestruturas de ZnO são usadas em sistemas de dispositivos, como fotodetectores, sensores de gás, dispositivos de fotoemissão, fotossensores UV e muitos outros em

optoeletrônica. No presente trabalho, estudamos filmes finos nanocristalinos de ZnO: Ga preparados por imersão em sol-gel. técnica de revestimento. As amostras foram caracterizadas por Difração de Raios-X de Incidência de Grazing (GIXD), refletividade de raios-X (XR) e dispersão de raios-X de pequeno ângulo de incidência pastosa Métodos (GISAXS) e Microscopia Eletrônica de Varredura de Efeito de Campo (FESEM). A caracterização das amostras mostra que os filmes obtidos eram uniformes, contínuos, com tamanho de cristalito em torno de 12 nm, tamanho médio dos poros em torno de 3,5 nm e fração volumétrica de nanoporosidade entre 0,18 e 0,3. A comparação de densidades entre filmes dopados e não dopados é discutida.

Palavras-chave: ZnO: Ga, filmes nanocristalinos, GISAXS, XR.

1 INTRODUCTION

ZnO based films have been actively studied because of their applications as solar cells, gas sensors, piezoelectric transducers, ultrasonic oscillators and for different optoelectronic applications. Besides their interesting optical, electrical and piezoelectrical properties, this material exhibits a high chemical and mechanical stability. ZnO presents novel properties and potential applications in optoelectronic fields because its non linear optical properties, excitonic emission at room temperature and quantum size effect[1,2].

Doping with gallium can increase the conductivity by one or two orders of magnitude and its similar ionic radius to zinc could result in only small ZnO lattice deformations even at higher Ga concentrations [3].

2 EXPERIMENTAL

Ga-doped ZnO films were obtained using the sol-gel method, from a precursor solution prepared with 3% gallium nitrate in zinc acetate dihydrate (0.2M) dissolved in 2-methoxyethanol. Solution was deposited over amorphous SiO₂ substrates through spin-coating techniques at 3000 rpm for 10s. After the deposition of each layer, drying process at 200°C during 10 min was carried out in order to consolidate the deposited material. Films with 2, 4, 6 and 8 layers were prepared (labeled as ZnO:Ga-*n* with *n*=2,4,6,8 respectively). All the samples received a final thermal treatment, necessary for crystallization and the elimination of organic residues, at 450°C for 3 hours.

Obtaining of crystalline ZnO nanostructures on all samples was verified by Grazing Incidence X-ray Diffraction (GIXD), at a constant grazing incidence angle ($\alpha_i = 1^\circ$). An Empyrean Panalytical diffractometer, with Cu K α radiation ($\lambda = 1.5442 \text{ \AA}$), and a PIXCEL 3D detector, were used for this purpose at the X-Rays Diffraction Laboratory,

Condensed Matter Physics Department, Research and Applications, GAIyANN - CAC - CNEA (Buenos Aires, Argentina).

All the films were studied by XR and GISAXS at the XRD2 line of the National Laboratory of Synchrotron Light (LNLS), Campinas, Brazil, using a monochromatic 8 keV ($\lambda = 1.549\text{\AA}$) photon beam.

XR measurements were carried out by varying the grazing incidence angle (α) between 0.1° and 2° . Using XR technique we derived the average film densities from the values of the critical angle (α_c) of total X-ray reflection [6,9]. The lack of definition of the Kiessig fringes [4] made that the thickness of the sample could not be determined by this technique.

The GISAXS technique was applied to determine the shape and the size distribution of nanopores embedded in the thin films. The grazing incidence angle of the X-ray beam was set at 0.35° for all the studied samples. The GISAXS intensities recorded in 2D images were attributed to the diffusion produced by dispersed nanopores in the studied films. The analysis of the GISAXS intensity was performed using the IsGisaxs 2.6 program [5]. The contributions were modeled by the distorted wave Born approximation (DWBA) with a model of spheroidal pores [6,7]. We also compare the present pore distribution results with those obtained in a previous work [8].

General features and thicknesses of the films were observed by Field Emission Scanning Electron Microscopy (FESEM) at the Advanced Microscopy Center (FCEyN-UBA, Argentina).

3 RESULTS

1. GIXD

Figure 1 shows the GIXD diffraction patterns of the ZnO:Ga-*n* films. The main peaks corresponding to reflections of the planes (100) (002) and (101) in ZnO-wurtzite crystals can be seen in the range $2\theta = [30^\circ-40^\circ]$.

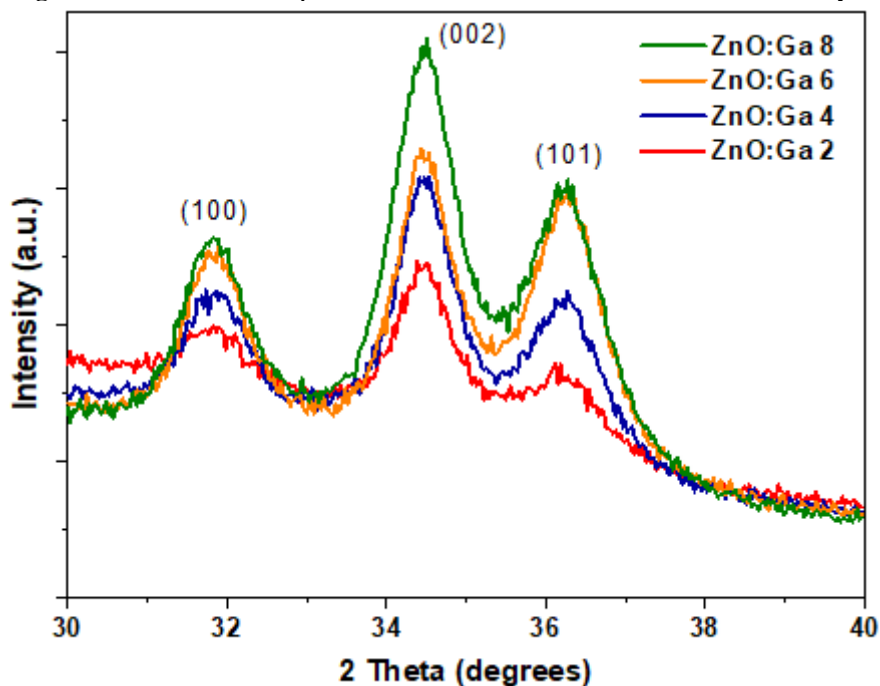
The increasing total area below the peaks verifies an increasing thickness of the films with the number of layers.

ZnO crystallites size (D) of the film was estimated by Scherrer equation:

$$D = 0.9\lambda / (B\cos\theta_B)$$

Where B is the integral breadth (in radians) and θ_B the Bragg angle of the diffraction peak [9]. An average size value obtained from the three peaks was considered in each film. These values are shown in Table 1.

Fig 1: GIXRD Diffraction patterns of ZnO:Ga-*n* films with *n* = 2,4,6 and 8 layers

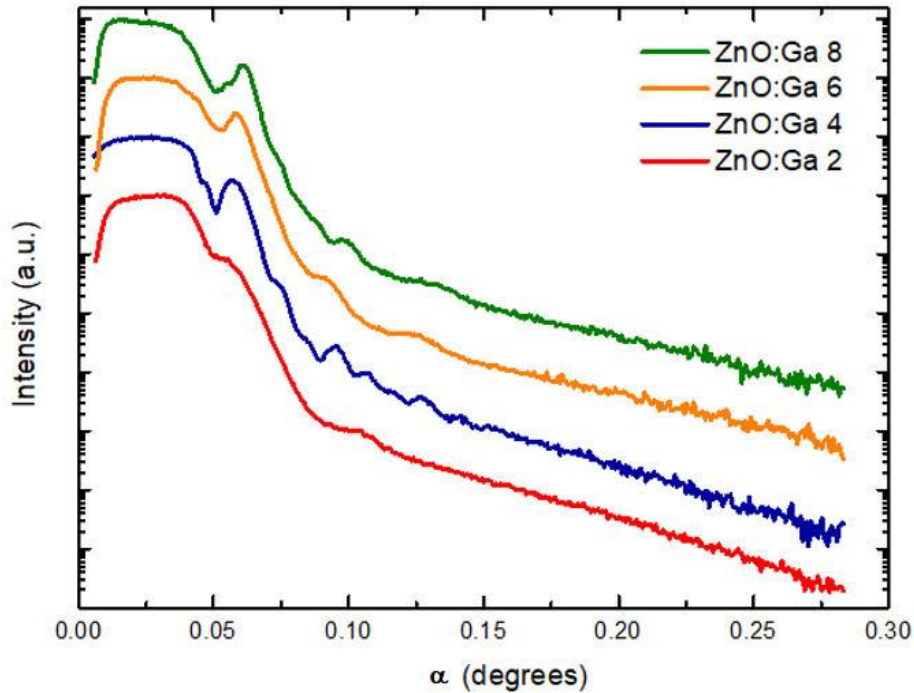


2 XR

Figure 2 shows the experimental XR reflectivity diagrams of the studied films, where the intensity of the radiation (log scale) is plotted as function of the grazing incidence angle α . They were corrected by the geometric factors (height of the incident beam and length of the sample) at small incidence angles (rectified region) [4,10] and normalized with the maximum intensity. The curves corresponding to films with different number of layers are vertically shifted for clarity.

It can be seen that the obtained curves do not present the expected fringes, for this reason the thicknesses determination of the thin films were not achieved by this technique. Films densities (ρ) and volumen fraction of the porosity (p) were determined by critical angle measurement [8,11]. Results are shown in Table 2.

Fig. 2 X-ray reflectivity intensity corresponding to the ZnO:Ga-*n* films with *n* = 2, 4, 6 and 8 layers



3 GISAXS

In Figure 3 it can be seen as an example: (a) the ZnO:Ga-6 GISAXS 2D image and (b) the experimental (open red circles) and modeled (black solid lines) transmitted intensity profiles, for fixed values of the exit angle α_f , as a function of the modulus of the in-plane component ($q_{//}$) of scattering vector \vec{q} , defined as [5]:

$$\vec{q} = \vec{k}_f - \vec{k}_i = \frac{2\pi}{\lambda} \begin{pmatrix} \cos 2\theta \cos \alpha_f - \cos \alpha_i \\ \sin 2\theta \cos \alpha_f \\ \sin \alpha_f + \sin \alpha_i \end{pmatrix}$$

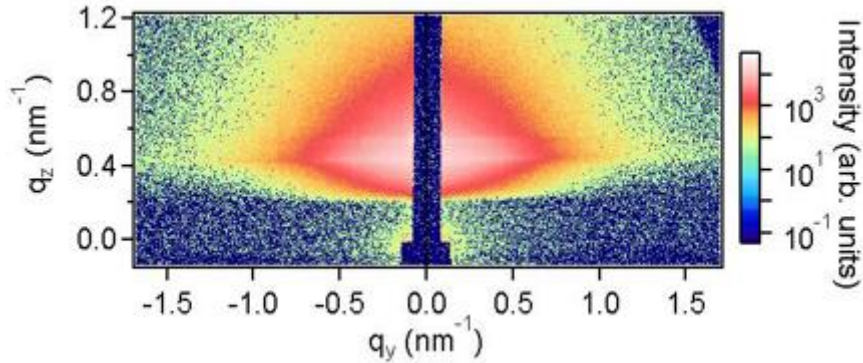
$$q_{//} = \frac{2\pi}{\lambda} [(\cos 2\theta \cos \alpha_f - \cos \alpha_i)^2 + (\sin 2\theta \cos \alpha_f)^2]^{1/2}$$

λ being the X-ray wavelength, 2θ the horizontal scattering angle and α_f the angle between the scattered X-ray beam and the surface of the sample.

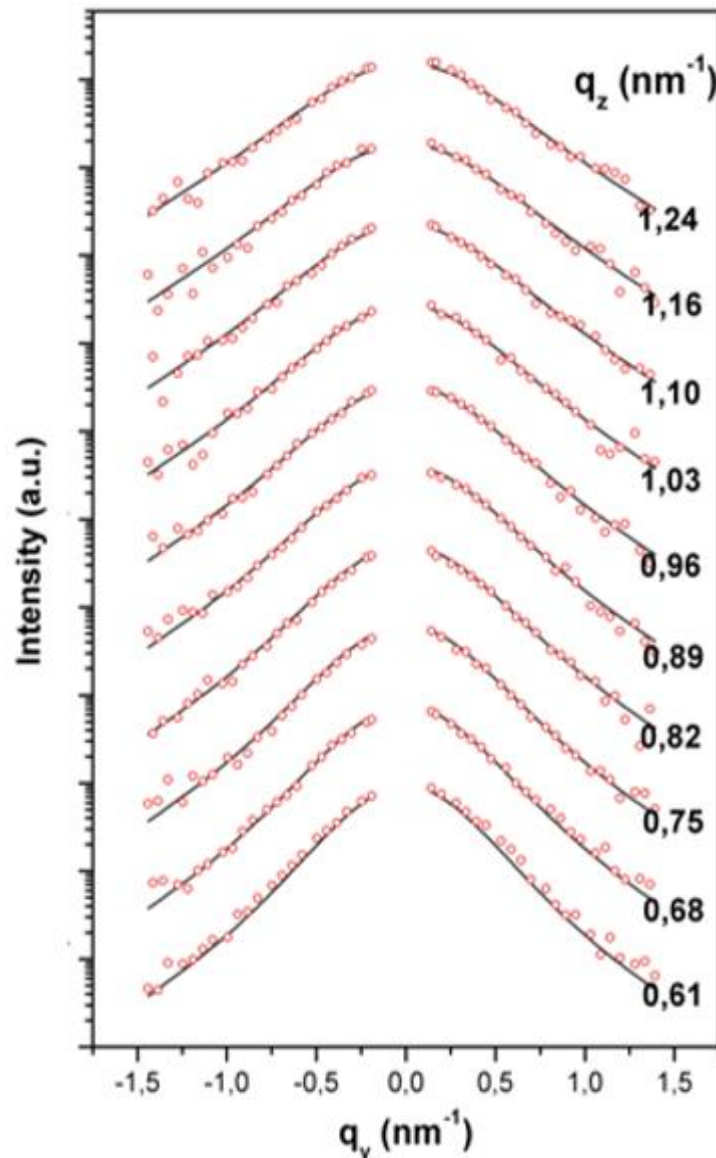
The values resulting from the IsGISAXS adjustments, corresponding to the height/width aspect ratio (v), the average pore radius in the film plane direction ($\langle R \rangle$) and the size dispersion (standard deviation) of the nanopores radius (σ_R), are shown in Table 1. This table also includes pure ZnO samples grown with a similar method, for comparison [8].

For each sample, critical angle was estimated from the Yoneda Peak in the corresponding 2D image [12-14]. Films densities (ρ) and volume fraction of the porosity (p) were determined by these critical angle values [8] (Table 2).

Fig. 3 (a): 2D GISAXS Image corresponding to 6 layered film ZnO:Ga-6



3.b). 1D GISAXS intensity profiles extracted from 2D GISAXS intensity patterns of ZnO:Ga-6 film at the indicated q_z values (red circles) and best fitted curves (black solid lines). The curves were put one on top of the other for clarity.



4 FESEM

The images in Figure 4 show FESEM micrographs corresponding to the 6 layered film ZnO:Ga-6. In Fig.4.a) a continuous film with uniform texture and small grains can be observed, while Fig. 4.b) displays a cross section of the film where the thickness is indicated. Thicknesses films values obtained from the micrographs are shown in Table 1.

Fig 4: Micrographs FESEM corresponding to a 6 layered film: a) Surface image; b) Cross section (yellow line indicates the film thickness).

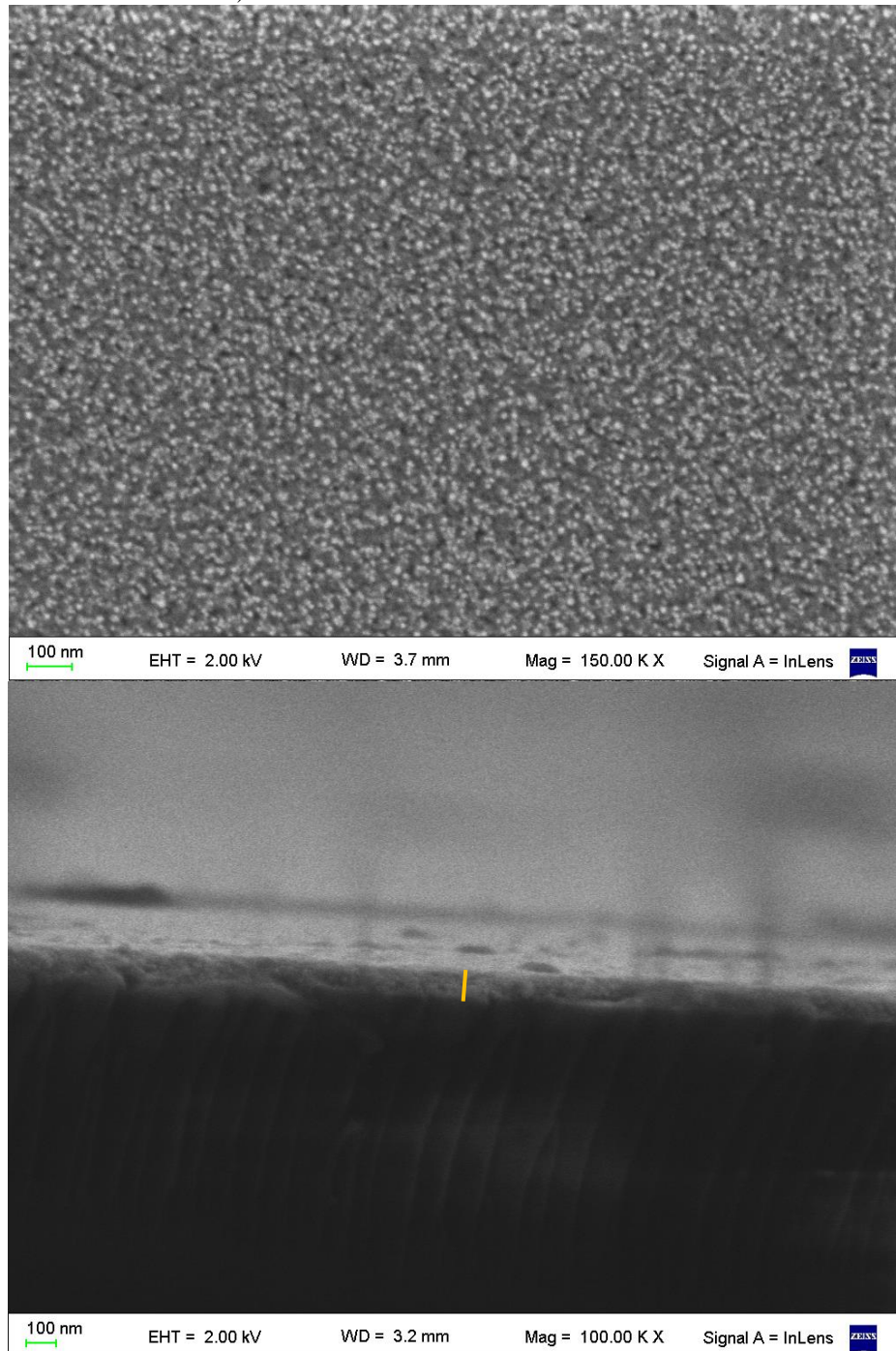


Table 1. Parameters obtained from the ZnO:Gafilm with different numbers of deposited layers (n) characterized by different techniques (GIXD, FESEM and GISAXS). D is the average ZnO crystallite diameter, t the film thickness, ν the height/width aspect ratio, $\langle R \rangle$ the average pore radius in the film plane direction and σ_R the size dispersion (standard deviation) of the nanopores radius. Table includes pure ZnO samples grown with a similar method, for comparison [8].

Sample	n	GIXD	FESEM	GISAXS		
		D (nm)	t (nm)	ν	$\langle R \rangle$ (nm)	σ_R (nm)
ZnO:Ga-2	2	12	38	0.92	3.81	1.29
ZnO:Ga-4	4	12	50	0.86	3.30	1.22
ZnO:Ga-6	6	12	92	0.88	3.65	1.45
ZnO:Ga-8	8	12	115	0.87	3.23	1.25
ZnO-2	2	20	---	0.88	4.98	2.20
ZnO-4	4	23	86	0.80	6.88	2.65
ZnO-6	6	28	107	0.83	6.60	2.50
ZnO-8	8	23	146	0.88	6.10	1.97

Table 2. Critical angle (α_c), average mass density (ρ) and volume fraction of the nanoporosity (p) obtained by XR and GISAXS, corresponding to the ZnO:Ga films. The mass density derived from GISAXS image was determined from the position of α_f of the Yoneda peak. Table includes pure ZnO samples grown with a similar method, for comparison [8].

Sample	n	XR			GISAXS (Yonedapeak)		
		α_c (degrees)	ρ (g/cm ³)	p	α_c (degrees)	ρ (g/cm ³)	p
ZnO:Ga-2	2	0.295	4.55	0.19	0.249	3.24	0.42
ZnO:Ga-4	4	0.297	4.62	0.18	0.239	2.99	0.47
ZnO:Ga-6	6	0.296	4.58	0.18	0.268	3.77	0.33
ZnO:Ga-8	8	0.274	3.93	0.30	0.268	3.77	0.33
ZnO-2	2	0.300	4.71	0.16	0.300	4.71	0.16
ZnO-4	4	0.261	3.56	0.36	0.260	3.54	0.36
ZnO-6	6	0.279	4.09	0.27	0.260	3.54	0.36
ZnO-8	8	0.263	3.62	0.35	0.263	3.62	0.35

5 CONCLUSIONS

In the present work ZnO:Ga thin films (2, 4, 6 and 8 layers) were obtained. The density and pores structure were studied by XR and GISAXS. The values obtained were compared with previous results of pure ZnO.

Crystallite sizes were lower in Ga doped films than in pure ZnO, being for the doped ones a uniform size of 12nm, regardless of the number of layers, while the pure ones have sizes between 20 and 28nm.

The average pore radius and the size dispersion were also found to be lower in doped films. In the studied samples, the radii of the pores stay in the range of [3.2; 3.8] nm and the dispersion between [1.22; 1.45], while the pure ZnO samples show pores between [4.98, 6.10] nm with dispersions in the range of [1.97; 2.65].

The aspect ratio of the doped films pores range between 0.86 and 0.92, and for pure films between 0.80 and 0.88. Pores are more flattened along the direction normal to the substrate surface in pure films than in doped ones.

Densities obtained by the critical angle from XR curves are greater or equal than those obtained by the critical angle from GISAXS 2D images, being in all cases values lower than the bulk ZnO density. Comparison of densities between doped and undoped films do not present a clear relationship.

FESEM images of ZnO:Ga films show uniform and continuous surfaces in all samples. Thicknesses increase with the number of layers. Doped films are thinner than undoped ones.

REFERENCES

1. [1] A.B.Djurišić, A.M.C.Ng, X.Y.Chen, *ZnO nanostructures for optoelectronics: Material properties and device Applications*, Progress in Quantum Electronics Volume 34, Issue 4 (2010) 191-259.
 - [2] Ü. Özgür, Y. I.Alivov, C. Liu, A.M. Teke, A. Reshchikov, S. Doğan, V. Avrutin, S. J. Cho, H. J. Morkoç, *A comprehensive review of ZnO materials and devices*, Appl. Phys. 200598(4), 41301.
 - [3] S. J. Henley, M. N. R. Ashfold, D. Cherns, Surf. Coat. Technol. 2004, 177, 271
 - [4] M. Tolan, *X-ray Scattering from Soft-matter Thin Films*, Springer, Berlin Heidelberg/New York, 1999.
 - [5] R. Lazzari, J. Appl. Crystallogr. 35 (2002) 406-421.
 - [6] K. Stoev, and K. Sakurai, Review on grazing incidence X-ray spectrometry and reflectometry, Spectrochimica Acta Part B 54, 1 (1999) 41-82.
 - [7] V. Holý, U. Pietsch, T. Baumbach, *High-Resolution X-Ray Scattering from Thin Films and Multilayers*, Springer-Verlag, Berlin, 1999.
 - [8] E. Heredia, C. Bojorge, J. Casanova, H. Cánepa, A. Craievich, G. Kellermann, Nanostructured ZnO thin films prepared by sol-gel spin-coating, Applied Surface Science 317 (2014) 19-25.
 - [9] H.P. Klug, L.E. Alexander, *X-ray Diffraction Procedures for Polycrystalline and Amorphous Materials*, John Wiley & Sons, New York, 1974.
 - [10] A. Gibaud, G. Vignaud, S.K. Sinha, *The correction of the geometrical factor in the analysis of X-ray reflectivity*, Acta Crystallogr. A 49 (1993) 642-648.
 - [11] J. Bolze, M. Ree, H.S. Youn, S. Chu, K. Char, *Synchrotron X-ray reflectivity study on the structure of templated polyorganosilicate thin films and their derived nanoporous analogues*, Langmuir 17 (2001) 6683-6691.
 - [12] J.R. Casanova, E.A. Heredia, C.D. Bojorge, H.R. Cánepa, G. Kellermann, A.F. Craievich, *Structural characterization of supported nanocrystalline ZnO thin films prepared by dip-coating*, Appl. Surf. Sci. 257 (2011) 10045-10051.
 - [13] G. Renaud, R. Lazzari, F. Leroy, *Probing surface and interface morphology with Grazing Incidence Small Angle X-Ray Scattering*, Surf. Sci. Rep. 64 (2009) 255-380. <https://doi.org/10.1016/j.surfrep.2009.07.002>.
 - [14] K. Hoydalsvik, T. Barnardo, R. Winter, S. Haas, D. Tatchev and A. Hoell; Phys. Chem. Chem. Phys. 12 (2010) 14492-14500.
- Acknowledgements:** Authors are grateful to MINDEF, CONICET (Argentina) and LNLS (Brazil) for the grants received for the realization of this work.